Available online at www.sciencedirect.com
SCIENCE DIRECT
Journal of Organometallic Chemistry 691 (2006) 309–322
Journal of Organometallic Chemistry
www.elsevier.com/locate/jorganchem

Dppm-substituted ruthenium clusters with capping sulfido and selenido ligands derived from thiourea, tetramethylthiourea and elemental selenium

Syed J. Ahmed [a], Md. Iqbal Hyder [a], Shariff E. Kabir [*,a], Md. Arzu Miah [a], Antony J. Deeming [b,*], Ebbe Nordlander [*,c]

[a] Department of Chemistry, Jahangirnagar University, Savar, Dhaka 1342, Bangladesh
[b] Department of Chemistry, University College London, 20 Gordon Street, London WC 1H OAJ, UK
[c] Inorganic Chemistry, Center for Chemistry and Chemical Engineering, Lund University, P.O. Box 124, S-22100 Lund, Sweden

Received 9 August 2005; accepted 12 August 2005
Available online 20 October 2005

Abstract

Treatment of $[Ru_3(CO)_{10}(\mu\text{-dppm})]$ (**4**) [dppm = bis(diphenylphosphido)methane] with tetramethylthiourea at 66 °C gave the previously reported dihydrido triruthenium cluster $[Ru_3(\mu\text{-H})_2(\mu_3\text{-S})(CO)_7(\mu\text{-dppm})]$ (**5**) and the new compounds $[Ru_3(\mu_3\text{-S})_2(CO)_7(\mu\text{-dppm})]$ (**6**), $[Ru_3(\mu_3\text{-S})(CO)_7(\mu_3\text{-CO})(\mu\text{-dppm})]$ (**7**) and $[Ru_3(\mu_3\text{-S})\{\eta^1\text{-C}(NMe_2)_2\}(CO)_6(\mu_3\text{-CO})(\mu\text{-dppm})]$ (**8**) in 6%, 10%, 32% and 9% yields, respectively. Treatment of **4** with thiourea at the same temperature gave **5** and **7** in 30% and 10% yields, respectively. Compound **7** reacts further with tetramethylthiourea at 66 °C to yield **6** (30%) and a new compound $[Ru_3(\mu_3\text{-S})_2\{\eta^1\text{-C}(NMe_2)_2\}(CO)_6(\mu\text{-dppm})]$ (**9**) (8%). Thermolysis of **8** in refluxing THF yields **7** in 55% yield. The reaction of **4** with selenium at 66 °C yields the new compounds $[Ru_3(\mu_3\text{-Se})(CO)_7(\mu_3\text{-CO})(\mu\text{-dppm})]$ (**10**) and $[Ru_3(\mu_3\text{-Se})(\mu_3\text{-}\eta^3\text{-PhPCH}_2\text{PPh}(C_6H_4)\}(CO)_6(\mu\text{-CO})]$ (**11**) and the known compounds $[Ru_3(\mu\text{-H})_2(\mu_3\text{-Se})(CO)_7(\mu\text{-dppm})]$ (**12**) and $[Ru_4(\mu_3\text{-Se})_4(CO)_{10}(\mu\text{-dppm})]$ (**13**) in 29%, 5%, 2% and 5% yields, respectively. Treatment of **10** with tetramethylthiourea at 66 °C gives the mixed sulfur-selenium compounds $[Ru_3(\mu_3\text{-S})(\mu_3\text{-Se})(CO)_7(\mu\text{-dppm})]$ (**14**) and $[Ru_3(\mu_3\text{-S})(\mu_3\text{-Se})\{\eta^1\text{-C}(NMe_2)_2\}(CO)_6(\mu\text{-dppm})]$ (**15**) in 38% and 10% yields, respectively. The single-crystal XRD structures of **6**, **7**, **8**, **10**, **14** and **15** are reported.

Keywords: Triruthenium clusters; Tetramethylthiourea; Sulfur; Selenium; Carbene; Alkylidene; X-ray structures

1. Introduction

Reactions between thioureas and transition metal carbonyl clusters of ruthenium [1–9] and osmium [10–12] have been extensively studied, initially by the Süss-Fink group [1–9]. These reactions are generally accompanied by cleavage of N–H, C–N, C=S and C–H bonds depending upon the substituted thiourea and reaction conditions. For example, thiourea, dimethylthiourea and diphenylthiourea with $[Ru_3(CO)_{12}]$ lead to $[Ru_3(\mu\text{-H})(\mu_3\text{-}\eta^2\text{-RNCSNRH})(CO)_9]$ (Scheme 1), containing triply-bridging thioureato ligands by N–H bond cleavage [1].

In contrast, diisopropylthiourea and diethylthiourea react with $[Ru_3(CO)_{12}]$ under more forcing conditions to give tetraruthenium clusters, containing sulfido and diaminocarbene ligands (Scheme 2) by cleavage of the C=S bond [3].

Further variations are found in the treatment of di-*tert*-butylthiourea with $[Ru_3(CO)_{12}]$ at room temperature to give $[Ru_3(\mu\text{-H})(\mu_3\text{-S})(\eta^2\text{-CH}_2\text{CMe}_2\text{NHCNHBu}^t)(CO)_8]$ and $[Ru_3(\mu\text{-H})\{\mu_3\text{-SRu}(CO)_3\}(\eta^2\text{-CH}_2\text{CMe}_2\text{NHCNHBu}^t)(CO)_9]$ in which both C=S and C–H bonds are cleaved, leaving coordinated S and carbene ligands [6]. On the other hand,

* Corresponding author.
E-mail address: a.j.deeming@ucl.ac.uk (A.J. Deeming).

0022-328X/$ - see front matter © 2005 Elsevier B.V. All rights reserved.
doi:10.1016/j.jorganchem.2005.08.017

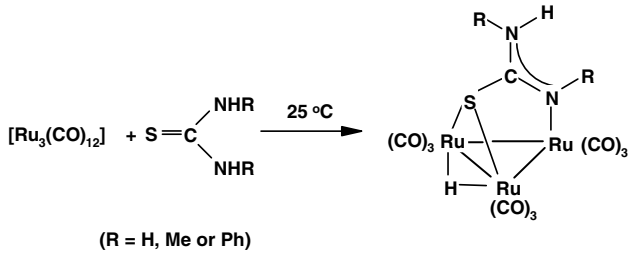

Scheme 1.

tetramethylthiourea reacts with $[Ru_3(CO)_{12}]$ at 66 °C to give two isomers of $[Ru_3(\mu\text{-}H)(\mu_3\text{-}S)(CH_2NMeCNMe_2)(CO)_8]$ with the organic group either bridging or chelating, as well as corresponding tetranuclear clusters [3].

Lewis et al. [10] and we [11,12] have investigated reactions of the reactive triosmium cluster $[Os_3(CO)_{10}(MeCN)_2]$ with thiourea, phenylthiourea and diphenylthiourea and obtained triosmium clusters of the type $[Os_3(\mu\text{-}H)(\mu\text{-}\eta^2\text{-}RNCSNHR)(CO)_{10}]$ and $[Os_3(\mu\text{-}H)(\mu_3\text{-}\eta^2\text{-}RNCSNHR)(CO)_9]$ containing edge- and triply-bridging thioureato ligands, respectively. In contrast, tetramethylthiourea reacts with $[Os_3(CO)_{12}]$ in the presence of $Me_3NO \cdot 2H_2O$ giving $[Os_3(CO)_{11}\{\eta^1\text{-}SC(NMe_2)_2\}]$, $[Os_3(\mu\text{-}OH)(\mu\text{-}MeOCO)\{\eta^1\text{-}SC(NMe_2)_2\}(CO)_9]$ and $[Os_3(\mu\text{-}H)(\mu_3\text{-}S)(\mu\text{-}MeOCO)\{\eta^1\text{-}SC(NMe_2)_2\}(CO)_8]$ containing S-coordinated tetramethylthiourea ligands [12]. We recently began systematic investigations of tetramethylthiourea reactivity with unsaturated triosmium clusters for which a variety of ligand coordination modes and transformations have been demonstrated including η^1-S-coordination, the latter being useful for further transformation [13]. Most recently we have investigated the reaction of tetramethylthiourea with the dppm-bridging triosmium cluster $[Os_3(CO)_{10}(\mu\text{-dppm})]$ (**1**) and obtained only $[Os_3(\mu_3\text{-}S)_2(CO)_7(\mu\text{-dppm})]$ as two separable isomers [14] (Scheme 3).

These compounds are potential building blocks for higher nuclearity clusters [15]. Naturally, we wished to compare such reactivity patterns for osmium with that of the ruthenium analogue **4**, which has also attracted attention for its reactivity with various small organics and for the role of dppm in stabilizing the cluster [16–27]. In this context, we describe in this paper the reactions of **4** with tetramethylthiourea, thiourea and elemental selenium.

2. Results and discussion

2.1. Synthesis

Cluster **4** reacts with tetramethylthiourea in refluxing THF to give, after chromatography, four triruthenium clusters: the known compound $[Ru_3(\mu\text{-}H)_2(\mu_3\text{-}S)(CO)_7(\mu\text{-dppm})]$ (**5**) (6%), and the new compounds $[Ru_3(\mu_3\text{-}S)_2(CO)_7(\mu\text{-dppm})]$ (**6**), $[Ru_3(\mu_3\text{-}S)(CO)_7(\mu_3\text{-}CO)(\mu\text{-dppm})]$ (**7**) and $[Ru_3(\mu_3\text{-}S)\{\eta^1\text{-}C(NMe_2)_2\}(CO)_6(\mu_3\text{-}CO)(\mu\text{-dppm})]$ (**8**) in 10%, 32% and 9% yields, respectively (see Scheme 4). We recently reported **5** from the treatment of **4** with H_2S and it was characterized by single-crystal XRD [28].

Treatment of **4** with thiourea in refluxing THF gives **5** and **7** in 30% and 10% yields, respectively. This observation is similar to that reported for the corresponding osmium analogue $[Os_3(CO)_{10}(\mu\text{-dppm})]$ which afforded $[Os_3(\mu\text{-}H)_2(\mu_3\text{-}S)(CO)_7(\mu\text{-dppm})]$ and $[Os_3(\mu_3\text{-}S)(\mu_3\text{-}CO)(CO)_7(\mu\text{-dppm})]$ when treated with thiourea at 110 °C [14].

Treatment of **7** with tetramethylthiourea in refluxing THF gives the new cluster $[Ru_3(\mu_3\text{-}S)_2\{\eta^1\text{-}C(NMe_2)_2\}(CO)_6(\mu\text{-dppm})]$ (**9**) together with compound **6** (Scheme 5) in 8% and 30% yields, respectively.

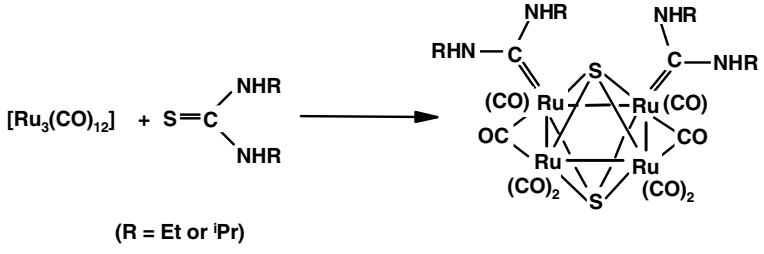

Scheme 2.

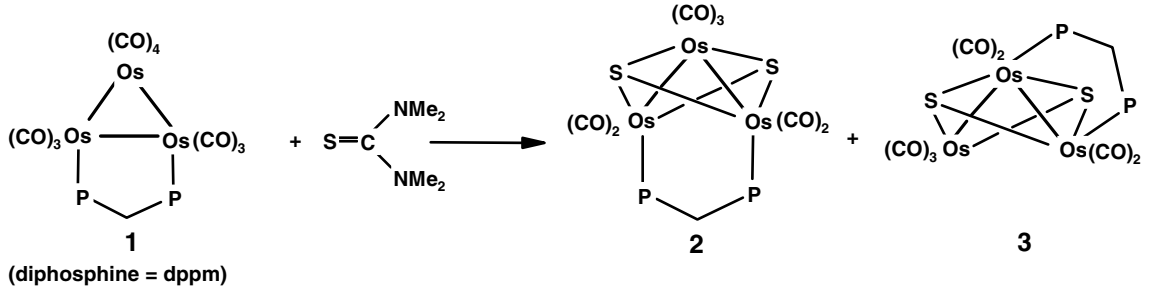

Scheme 3.

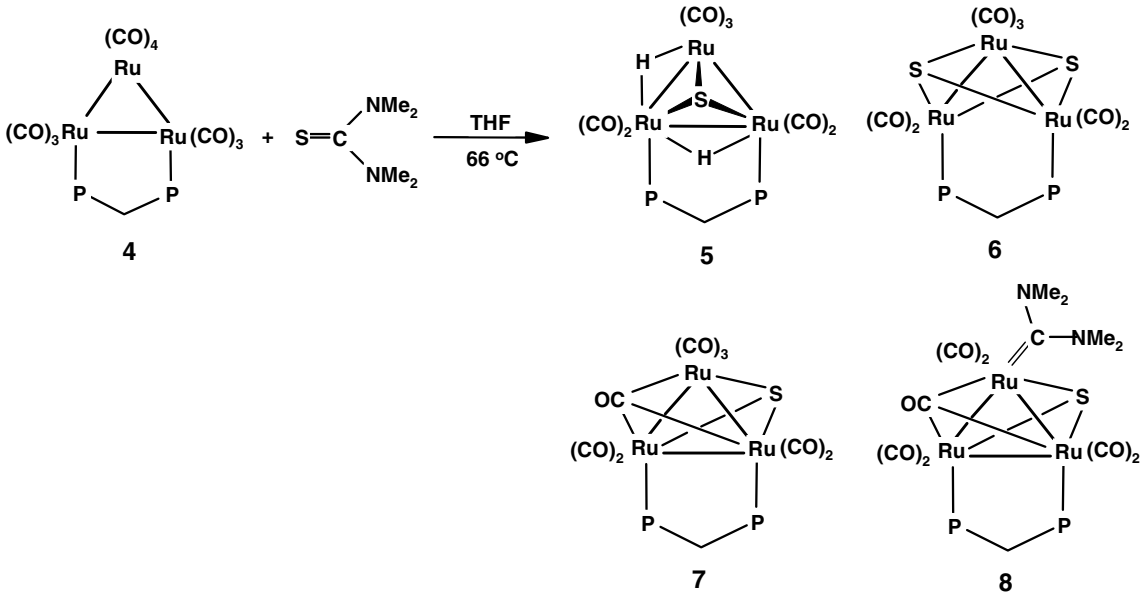

Scheme 4.

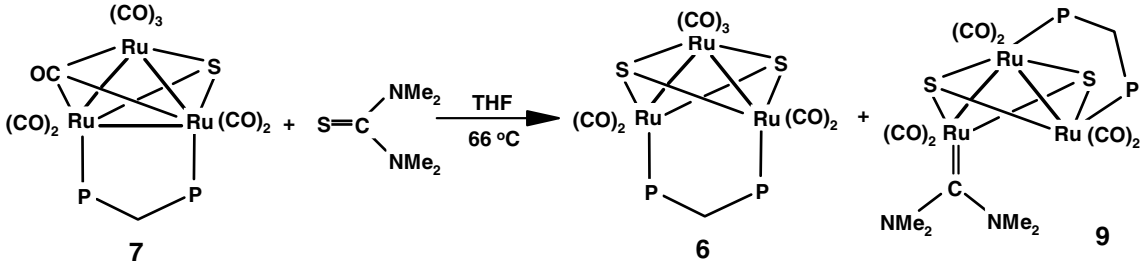

Scheme 5.

Treatment of **4** with elemental Se in refluxing THF at 66 °C produces two new clusters: $[Ru_3(\mu_3\text{-Se})(CO)_7(\mu_3\text{-CO})(\mu\text{-dppm})]$ (**10**) and $[Ru_3(\mu_3\text{-Se})(CO)_6(\mu\text{-CO})\{\mu_3\text{-}\eta^3\text{-PPhCH}_2\text{PPh}(C_6H_4)\}]$ (**11**) in 29% and 5% yields, respectively and two known compounds $[Ru_3(\mu\text{-H})_2(\mu_3\text{-Se})(CO)_7(\mu\text{-dppm})]$ (**12**) and $[Ru_4(\mu_3\text{-Se})(CO)_{10}(\mu\text{-dppm})]$ (**13**) in 2% and 5% yields, respectively (see Scheme 6). We [38] have recently reported **12** from hydrogenation of **10** while Predieri et al. [32] reported **13** from the reaction of $[Ru_3(CO)_{12}]$ with $dppmSe_2$.

The reaction of **10** with tetramethylthiourea at 66 °C yields two triruthenium mixed sulfur-selenium compounds $[Ru_3(\mu_3\text{-S})(\mu_3\text{-Se})(CO)_7(\mu\text{-dppm})]$ (**14**) and $[Ru_3(\mu_3\text{-S})(\mu_3\text{-Se})\{\eta^1\text{-C}(NMe_2)_2\}(CO)_6(\mu\text{-dppm})]$ (**15**) in 38% and 10% yields, respectively (see Scheme 7). The new compounds were characterized by elemental analysis, infrared, ^1H NMR, $^{31}P\{^1H\}$ NMR spectroscopy and MS data together with single-crystal XRD studies for **6**–**8**, **10**, **14**, and **15**.

2.2. XRD and spectroscopic studies

The structures of **6** (Fig. 1 and Table 1) and **14** (Fig. 2 and Table 2) consist of an 'open' trinuclear clusters with two metal–metal bonds [Ru(1)–Ru(2) = 2.8150(9) Å, Ru(1)–Ru(3) = 2.8217(9) Å for **6** and Ru(1)–Ru(2) = 2.8444(8) Å and Ru(1)–Ru(3) = 2.8373(8) Å for **14**], a nonbonded separation of 3.5802 Å for **6** and 3.626 Å for **14** along the Ru(2)–Ru(3) edge, seven terminal carbonyl groups, a μ_2-dppm and two μ_3-S for **6** and a μ_3-Se and a μ_3 S ligands for **14**. The metal–metal bond lengths are similar but very slightly shorter that those in $[Ru_3(CO)_{12}]$ [average 2.854(4) Å] [29] but are comparable to the Ru–Ru distances in $[Ru_3(\mu_3\text{-Se})_2(CO)_7(\mu\text{-dppa})]$ [2.831(1) and 2.842(1) Å] [30] and $[Ru_3(\mu_3\text{-Se})_2(CO)_7(\mu\text{-dppe})]$ [2.796(2) and 2.828(2) Å] [31]. The seven carbonyl groups are distributed so that two are attached to each Ru(2) and Ru(3) and three to Ru(1). The diaxially coordinated dppm ligand spans the nonbonded Ru–Ru edge. The Ru–P distances [Ru(2)–P(1) = 2.3040(17) Å and Ru(3)–P(2) = 2.3046(16) Å for **6** and Ru(3)–P(1) = 2.3014(18) Å, Ru(2)–P(2) = 2.2956(17) Å for **14**] are slightly shorter than those found in **4** [35]. The nonbonding Ru(2)···Ru(3) separations [3.5802 Å for **6** and 3.626 Å for **14**] are significantly shorter than the corresponding nonbonding separation in $[Ru_3(\mu_3\text{-Se})_2(CO)_7(\mu\text{-dppe})]$ (3.75 Å) [31] and $[Ru_3(\mu_3\text{-Se})_2(CO)_7(\mu\text{-dppf})]$ (3.87 Å) [31]. In **7**, the Ru–S

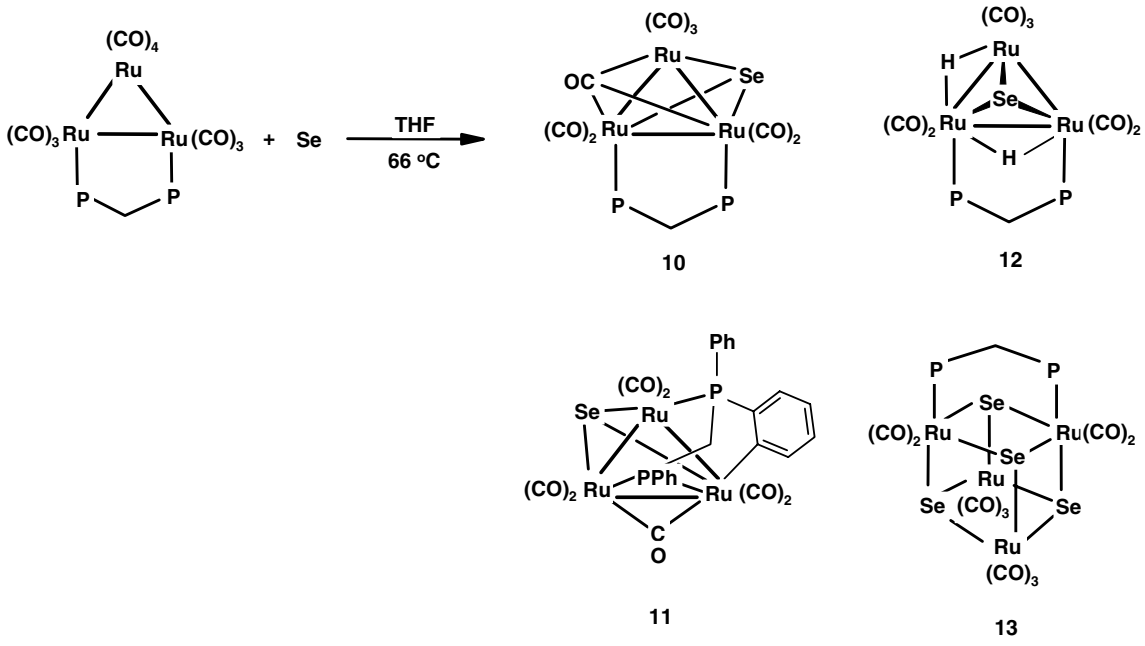

Scheme 6.

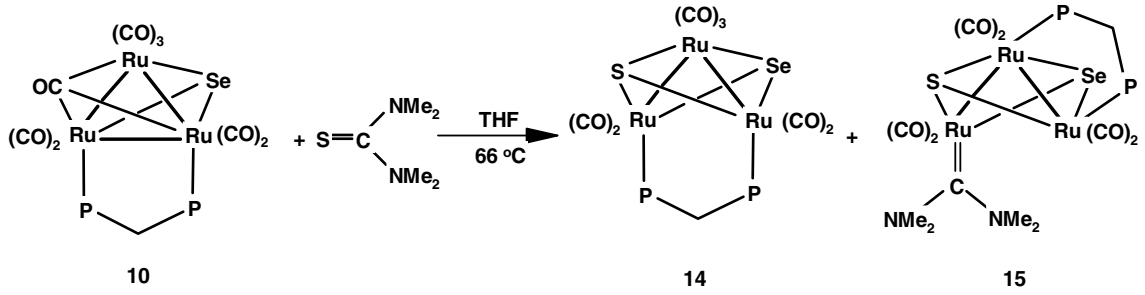

Scheme 7.

distances to the central 7-coordinate ruthenium atom Ru(1) [Ru(1)–S(1) = 2.4059(17) Å, Ru(1)–S(2) = 2.4244(17) Å] are longer than those to the external 6-coordinate ruthenium atoms [2.3729(18)–2.3924(18) Å]. In **14**, there is some disorder between the S and Se atoms with one site occupied by 0.83 Se and 0.17 S with the reverse in the other site. Fig. 2 shows the major occupancy labelled as Se(1) and S(1) and the minor as Se(1′) and S(1′). Although the μ_3-selenido triruthenium complexes $[Ru_3(\mu_3\text{-}Se)_2(CO)_7(\mu\text{-}PP)]$ (PP = dppm [32,33], dppf [31], dppe [31], dppa [30] have been reported, compounds **6** and **14** provide the first S mixed S, Se analogues.

The spectroscopic data of **6** are consistent with the solid-state structure. The MS shows the molecular ion (*m/z* 949) and the loss of seven carbonyl groups. The ^1H NMR spectrum contains a triplet at δ 3.14 ($J = 10.0$ Hz) for the dppm methylene. The $^{31}P\{^1H\}$ NMR spectrum exhibits a singlet at δ 61.2 implying one isomer with equivalent P nuclei. The ν(CO) values for **6** (2054s, 2016s, 1984m, 1971m cm^{-1}) are very similar to those of $[Ru_3(\mu_3\text{-}Se)_2(CO)_7(\mu\text{-}dppa)]$ (2057vs, 2022m, 1988w, 1971w cm^{-1}) [30], also a single isomer with dppa bridging the open Ru–Ru edge, but quite different from those of $[Ru_3(\mu_3\text{-}Se)_2(CO)_7(\mu\text{-}dppm)]$ (2066vs, 2052m, 2007w, 1956w cm^{-1}), a 1:2 mixture of isomers in solution differing in the relative disposition of the diphosphine ligand [32]. In the major isomer dppm bridges a bonded Ru–Ru edge and in the minor isomer two nonbonded Ru atoms.

The mass spectrum of **14** shows the expected parent ion at *m/z* 995, confirming that it is $[Ru_3(\mu_3\text{-}S)(\mu_3\text{-}Se)(CO)_7(\mu\text{-}dppm)]$ and is not a mixture containing $[Ru_3(\mu_3\text{-}Se)_2(CO)_7(\mu\text{-}dppm)]$ and $[Ru_3(\mu_3\text{-}S)_2(CO)_7(\mu\text{-}dppm)]$. The $^{31}P\{^1H\}$ NMR spectrum shows the presence of two inseparable isomers differing in the distribution of the Ru–Ru bonds. The major isomer **14a** (90%) has the dppm bridging two Ru atoms not connected by a Ru–Ru bond and gives a singlet (δ 63.9) while the minor isomer **14b** (10%) gives two doublets (δ 24.8 and 15.9, $J = 94.0$ Hz) since the dppm is across a bonded Ru–Ru edge. We have not confirmed experimentally that these isomers are in equilibrium but in the light of earlier results on $[Ru_3(\mu_3\text{-}Se)_2(CO)_7(\mu\text{-}dppm)]$ [32] they are probably are (see Scheme 8). The

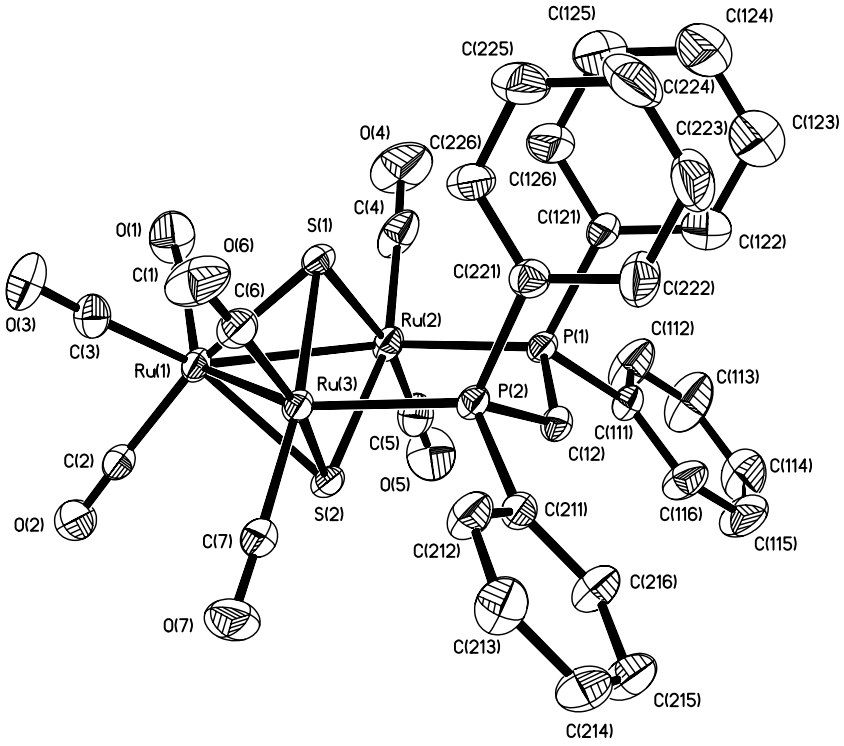

Fig. 1. Molecular structure of $[Ru_3(\mu_3\text{-}S)_2(CO)_7(\mu\text{-dppm})]$ (**6**).

IR spectrum is similar to that of $[Ru_3(\mu_3\text{-}Se)_2(CO)_7(\mu\text{-dppm})]$, supporting the presence of two isomers in solution.

The molecular structures of **7** and **10** are in Figs. 3 and 4, respectively, with data in Tables 3 and 4, respectively. There are two crystallographically independent but chemically equivalent molecules of **7**. The structures of **7** and **10** contain one μ_3-E, a μ-dppm, seven terminal carbonyl groups and a μ_3-carbonyl group, being formally derived from that of $[Ru_3(\mu_3\text{-}E)(CO)_9(\mu_3\text{-}CO)]$ [34] by replacement of an equatorial carbonyl group on each of the two Ru atoms by the dppm ligand. The complexes display tetrahedral Ru_3E cores with almost equilatorial Ru_3 triangles [Ru(1)–Ru(3) = 2.8103(13) Å, Ru(2)–Ru(3) = 2.8122 (15) Å and Ru(1)–Ru(2) = 2.7976(14) Å for **7** and Ru(2)–Ru(3) = 2.7964(3) Å, Ru(1)–Ru(3) = 2.8071(3) Å and Ru(1)–Ru(2) = 2.8184(3) Å for **10**] symmetrically capped by chalcogenido ligands [Ru(1)–S(1) = 2.362(3) Å, Ru(2)–S(1) = 2.369(3) Å and Ru(3)–S(1) = 2.368(3) Å for **7** and Ru(1)–Se(1) = 2.4844(4) Å, Ru(3)–Se(1) = 2.4901(4) Å and Ru(2)–Se(1) = 2.4935(4) Å for **10**]. Three of seven terminal carbonyl groups are bound to the Ru(1) atom and two to each of the other two Ru atoms. The triply-bridging carbonyl groups are asymmetrically attached [Ru(2)–C(1) = 2.105(11) Å, Ru(1)–C(1) = 2.273(10) Å and Ru(3)–C(1) = 2.204(11) Å for **7** and Ru(1)–C(8) = 2.242(3) Å, Ru(2)–C(8) = 2.157(3) Å and Ru(3)–C(8) = 2.150(3) Å for **10**]. The Ru-P bond distances [Ru(2)–P(1) = 2.334(3) Å and Ru(3)–P(2) = 2.367(3) Å for **7** and Ru(2)–P(1) = 2.3209(8) Å and Ru(3)–P(2) = 2.3336(8) Å for **10**] are comparable to those in **4** [2.322(2) and 2.334(2) Å] [35]. Chalcogenido compounds $[Ru_3(\mu_3\text{-}E)(CO)_7(\mu_3\text{-}CO)(\mu\text{-}PP)]$ (PP = dppm, dppe, dppa, dppf; E = S, Se, Te) have not previously been reported.

The mass spectra of **7** and **10** show the molecular ion peaks (*m*/*z* 945 for **7** and 991 for **10**) with successive loss of seven carbonyl groups, while IR and NMR spectra of **7** and **10** show the solid-state structures persist in solution. The IR carbonyl absorptions show a pattern similar to that reported for the corresponding osmium analogues $[Os_3(\mu_3\text{-}S)(CO)_7(\mu_3\text{-}CO)(\mu\text{-dppm})]$ [14] and $[Os_3(\mu_3\text{-}Se)(CO)_7(\mu_3\text{-}CO)(\mu\text{-dppm})]$ [38]. The presence of μ_3 carbonyl groups in **7** and **10** are apparent from the ν(CO) bands at 1736 cm^{-1} for **7** and 1655 cm^{-1} for **10**. The $^{31}P\{^1H\}$ NMR spectra contain a singlet at δ 25.6 for **7** and 25.9 for **10** indicating equivalent ^{31}P nuclei.

The molecular structure of **8** (Fig. 5 and Table 5) consists of a Ru_3 triangle with three metal–metal bonds [Ru(1)–Ru(2) = 2.7874(4) Å, Ru(1)–Ru(3) = 2.8151(4) Å and Ru(2)–Ru(3) = 2.8231(4) Å]. It is a structurally unique compound with seven terminal carbonyls and one triply bridging carbonyl, a capping S, and a tetramethyldiaminocarbene ligand. The structure of this molecule relates to that of **7** except for tetramethyldiaminocarbene ligand. The Me_2NCNMe_2 ligand formed by C=S bond cleavage of the tetramethylthiourea is coordinated equatorially at Ru(3). The Ru–carbene distance, Ru(3)–C(3) = 2.122(4) Å, is comparable to similar bonds in the tetraruthenium complexes $[Ru_4(\mu_4\text{-}S)_2(CO)_7(\mu\text{-}CO)_2\{(C(NMe_2)_2\}_2]$ [2.053(9) and 2.085(9) Å] [3] and $[Ru_4(\mu_4\text{-}S)_2(CO)_8(\mu\text{-}CO)_2\{(C(NMe_2)_2\}]$ [2.086(4) Å] [3] obtained by treating $[Ru_3(CO)_{12}]$ with tetramethylthiourea. The carbene C–N distances,

Table 1
Selected bond distances (Å) and angles (°) for $[Ru_3(\mu_3\text{-}S)_2(CO)_7(\mu\text{-}dppm)]$ (**6**)

Ru(1)–Ru(2)	2.8150(9)
Ru(1)–Ru(3)	2.8217(9)
Ru(2)–Ru(3)	3.5802(8)
Ru(1)–S(1)	2.4059(17)
Ru(1)–S(2)	2.4244(17)
Ru(2)–S(1)	2.3844(19)
Ru(2)–S(2)	2.3834(19)
Ru(3)–S(1)	2.3924(18)
Ru(3)–S(2)	2.3729(18)
Ru(2)–P(1)	2.3040(17)
Ru(3)–P(2)	2.3046(16)
P(1)–C(12)	1.866(7)
P(2)–C(12)	1.846(6)
Ru(2)–Ru(1)–Ru(3)	78.86(3)
Ru(2)–S(1)–Ru(1)	71.98(5)
Ru(3)–S(2)–Ru(2)	97.65(6)
Ru(2)–S(2)–Ru(1)	71.67(5)
Ru(2)–S(1)–Ru(3)	97.09(6)
Ru(1)–S(1)–Ru(3)	72.04(5)
Ru(1)–S(2)–Ru(3)	72.05(5)
S(1)–Ru(1)–Ru(3)	53.76(4)
S(1)–Ru(1)–Ru(2)	53.66(4)
S(1)–Ru(2)–Ru(1)	54.36(4)
S(1)–Ru(3)–Ru(1)	54.20(4)
S(2)–Ru(1)–Ru(2)	53.49(4)
S(2)–Ru(1)–Ru(3)	53.13(4)
S(2)–Ru(2)–Ru(1)	54.84(4)
S(2)-Ru (3)–Ru(1)	54.82(4)
S(1)–Ru(1)–S(2)	79.30(6)
S(1)–Ru(2)–S(2)	80.55(6)
S(1)–Ru(3)–S(2)	80.60(6)
P(1)–Ru(2)–S(2)	96.25(6)
P(2)–Ru(3)–S(1)	92.03(6)
P(1)–Ru(2)–Ru(1)	137.02(5)
P(2)–Ru(3)–Ru(1)	135.34(5)

Table 2
Selected bond distances (Å) and angles (°) for $[Ru_3(\mu_3\text{-}S)(\mu_3\text{-}Se)(CO)_7(\mu\text{-}dppm)]$ (**14**)

Ru(1)–Ru(3)	2.8373(8)
Ru(1)–Ru(2)	2.8444 (8)
Ru(1)–Se(1)	2.5240(9)
Ru(2)–Se(1)	2.4760(10)
Ru(3)–Se(1)	2.4756(10)
Ru(3)–P(1)	2.3014(18)
Ru(2)–P(2)	2.2956(17)
Ru(3)–S(1)	2.4182(16)
Ru(2)–S(1)	2.4262(15)
Ru(1)–S(1)	2.4328(13)
Ru(3)–Ru(1)–Ru(2)	79.31(2)
S (1)–Ru(1)–Ru(2)	54.06(4)
S(1)–Ru(1)–Ru(3)	53.97(4)
S(1)–Ru(2)–Ru(1)	54.28(3)
S(1)–Ru(3)–Ru(1)	54.45(3)
Se(1)–Ru(1)–Ru(3)	54.62(2)
Se(1)–Ru(1)–Ru(2)	54.54(2)
Se(1)–Ru(2)–Ru(1)	56.13(2)
Se(1)–Ru(3)–Ru(1)	56.23(2)
Ru(2)–Se(1)–Ru(1)	69.34(3)
Ru(3)–Se(1)–Ru(1)	69.14(3)
Ru(3)–Se(1)–Ru(2)	94.15(3)
Ru(3)–S(1)–Ru(2)	96.91(5)
Ru(2)–S(1)–Ru(1)	71.66(4)
Ru(3)–S(1)–Ru(1)	71.59(4)
P(1)–C(8)–P(2)	121.2(3)

C(33)–N(1) = 1.355(5) Å and C(33)–N(2) = 1.345(5) Å, are characteristic of terminally coordinated aminocarbenes [36,37]. The μ_3-S ligand symmetrically caps the Ru_3 triangle with Ru–S distances in the narrow range 2.3744(9)–2.3821(10) Å. The μ_3-CO group is also bonded symmetrically. The higher electron density at Ru(3) caused by the

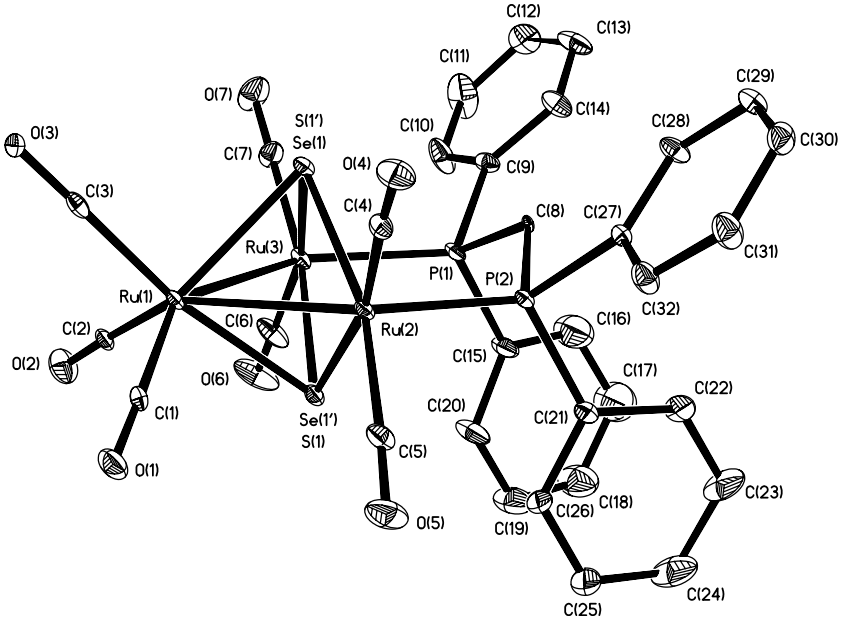

Fig. 2. Molecular structure of $[Ru_3(\mu_3\text{-}S)(\mu_3\text{-}Se)(CO)_7(\mu\text{-}dppm)]$ (**14**).

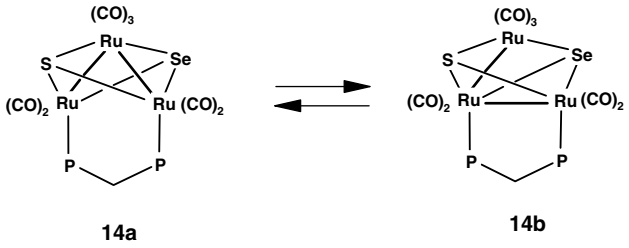

Scheme 8.

carbene ligand is most probably distributed over the whole ruthenium framework to result in nearly symmetrical carbonyl and S bridges in contrast to **7** where these bridges are unsymmetrical. The Ru–P distances in **8** [Ru(1)–P(1) = 2.3419(11) Å, Ru(2)–P(2) = 2.3211(11) Å] are comparable to those in **4** [35].

The IR spectrum of **8** shows a band at 1642 cm^{-1} for the μ_3-carbonyl ligand while the mass spectrum shows the molecular ion at m/z 1017 which loses seven carbonyl groups sequentially. The ^1H NMR spectrum contains three

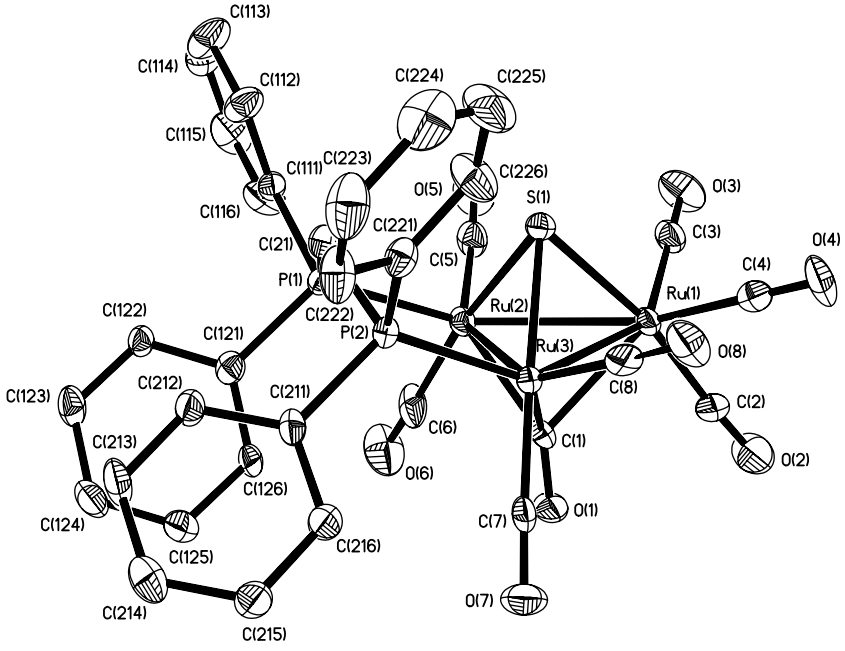

Fig. 3. Molecular structure of $[Ru_3(\mu_3\text{-}S)(CO)_7(\mu_3\text{-}CO)(\mu\text{-}dppm)]$ (**7**).

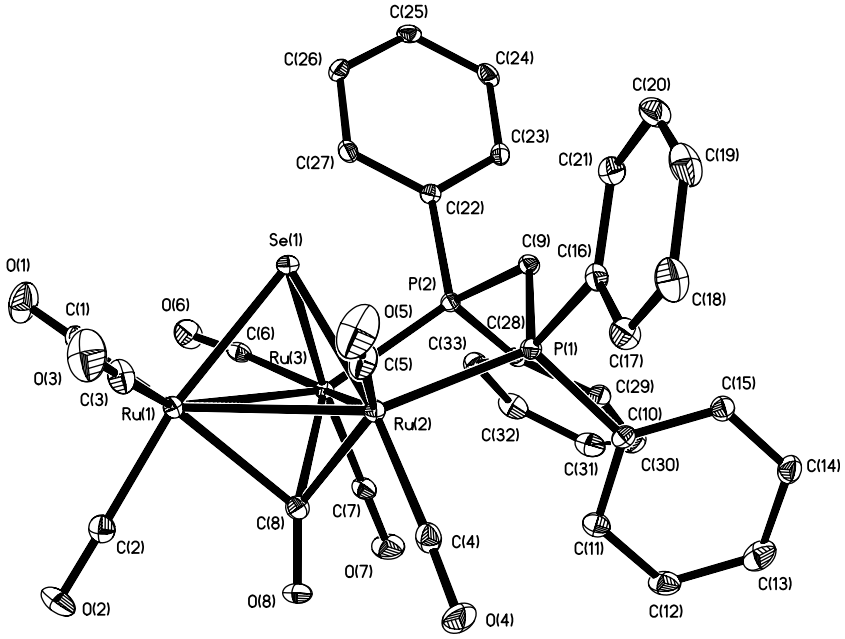

Fig. 4. Molecular structure of $[Ru_3(\mu_3\text{-}Se)(CO)_7(\mu_3\text{-}CO)(\mu\text{-}dppm)]$ (**10**).

Table 3
Selected bond distances (Å) and angles (°) for $[Ru_3(\mu_3\text{-}S)(CO)_7(\mu_3\text{-}CO)(\mu\text{-}dppm)]$ (**7**)

	Molecule **1**	Molecule **2**
Ru(1)–Ru(2)	2.7976(14)	2.8129(14)
Ru(1)–Ru(3)	2.8103(13)	2.8021(13)
Ru(2)–Ru(3)	2.8122(15)	2.8080(14)
Ru(1)–S(1)	2.362(3)	2.365(3)
Ru(2)–S(1)	2.369(3)	2.372(3)
Ru(3)–S(1)	2.368(3)	2.367(3)
Ru(1)–C(1)	2.273(10)	2.272(9)
Ru(2)–C(1)	2.105(11)	2.155(10)
Ru(3)–C(1)	2.204(11)	2.154(10)
Ru(2)–P(1)	2.334(3)	2.344(3)
Ru(3)–P(2)	2.367(3)	2.335(3)
S(1)–Ru(1)–Ru(2)	53.87(7)	53.68(7)
S(1)–Ru(2)–Ru(3)	53.57(7)	53.59(7)
S(1)–Ru(1)–Ru(3)	53.65(7)	53.72(7)
S(1)–Ru(3)–Ru(2)	53.60(7)	53.74(7)
S(1)–Ru(3)–Ru(1)	53.44(7)	53.67(7)
C(1)–Ru(1)–Ru(3)	50.0(3)	48.9(3)
C(1)–Ru(2)–Ru(3)	50.8(3)	49.3(3)
C(1)–Ru(3)–Ru(2)	47.7(3)	49.4(3)
C(1)–Ru(3)–Ru(1)	52.2(3)	52.6(3)
P(1)–Ru(2)–Ru(3)	92.08(8)	94.54(7)
P(2)–Ru(3)–Ru(2)	93.82(8)	92.92(7)

multiplets at δ 7.32, 3.88, 3.44 and a singlet at δ 3.26 in a relative intensity of 20:1:1:12 corresponding, respectively, to Ph, the non-equivalent CH_2 protons of dppm, and the Me of the carbene ligand. The $^{31}P\{^1H\}$ NMR spectrum contains a singlet at δ 28.5 indicating that the ^{31}P nuclei are equivalent. These solution data fit a structure like that found in the crystal.

Crystals of **9** suitable for XRD studies were unobtainable and spectroscopic data do not provide a unique structure.

Table 4
Selected bond distances (Å) and angles (°) for $[Ru_3(\mu_3\text{-}Se)(CO)_7(\mu_3\text{-}CO)(\mu\text{-}dppm)]$ (**10**)

Ru(1)–Ru(2)	2.8184(3)
Ru(1)–Ru(3)	2.8071(3)
Ru(2)–Ru(3)	2.7964(3)
Ru(1)–Se(1)	2.4844(4)
Ru(3)–Se(1)	2.4901(4)
Ru(2)–Se(1)	2.4935(4)
Ru(1)–C(8)	2.242(3)
Ru(3)–C(8)	2.150(3)
Ru(2)–C(8)	2.157(3)
Ru(2)–P(1)	2.3209(8)
Ru(3)–P(2)	2.3336(8)
P(1)–C(9)	1.844(3)
P(2)–C(9)	1.846(3)
Ru(3)–Ru(2)–Ru(1)	59.991(8)
Ru(3)–Ru(1)–Ru(2)	59.616(8)
Ru(2)–Ru(3)–Ru(1)	60.393(8)
Se(1)–Ru(2)–Ru(1)	55.364(10)
Se(1)–Ru(2)–Ru(2)	55.669(9)
Se(1)–Ru(3)–Ru(2)	55.925(9)
Se(1)–Ru(1)–Ru(3)	55.742(9)
Se(1)–Ru(3)–Ru(1)	55.551(10)
Se(1)–Ru(2)–Ru(3)	55.808(9)
C(8)–Ru(1)–Ru(3)	48.86(8)
C(8)–Ru(1)–Ru(2)	48.83(8)
C(8)–Ru(3)–Ru(2)	49.61(8)
C(8)–Ru(2)-Ru (3)	49.42(8)
C(8)–Ru(2)–Ru(1)	51.49(8)
Ru(1)–Se(1)–Ru(3)	68.707(11)
Ru(3)–Se(1)–Ru(2)	68.267(10)
Ru(1)–Se(1)–Ru(2)	68.968(11)
Ru(2)–C(8)–Ru(1)	79.68(10)
Ru(3)–C(8)–Ru(2)	80.97(11)
Ru(3)–C(8)–Ru(1)	79.42(10)
P(2)–Ru(3)–Ru(2)	96.688(19)
P(1)–Ru(2)–Ru(3)	89.53(2)
P(1)–C(9)–P(2)	113.55(16)

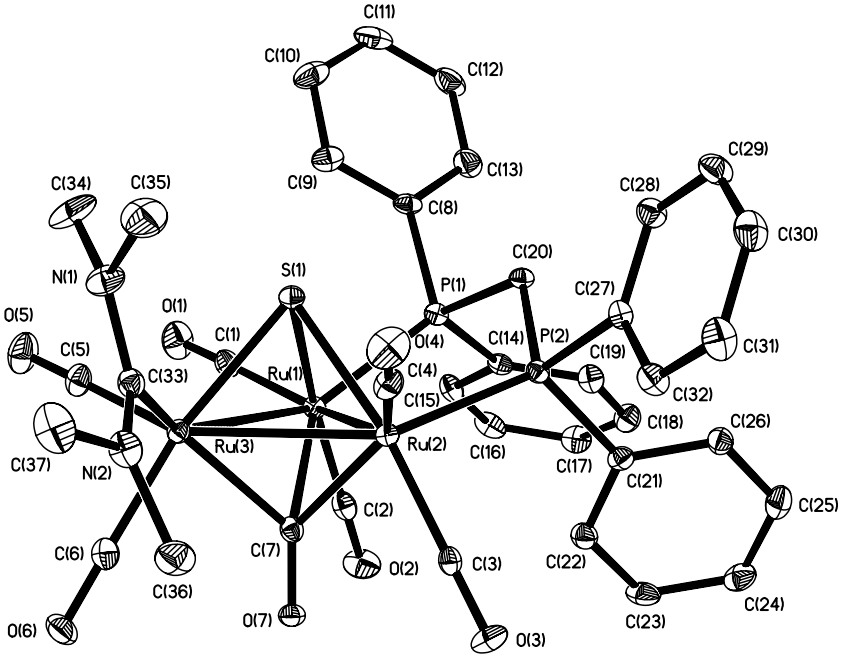

Fig. 5. Molecular structure of $[Ru_3(\mu_3\text{-}S)(CO)_6(\mu_3\text{-}CO)\{\eta^1\text{-}C(NMe_2)_2\}(\mu\text{-}dppm)]$ (**8**).

Table 5
Selected bond distances (Å) and angles (°) for $[Ru_3(\mu_3\text{-}S)\{\eta^1\text{-}C(NMe_2)_2\}(CO)_6(\mu_3\text{-}CO)(\mu\text{-}dppm)]$ (**8**)

Ru(1)–Ru(2)	2.7874(4)
Ru(1)–Ru(3)	2.8151(4)
Ru(2)–Ru(3)	2.8231(4)
Ru(1)–S(1)	2.3744(9)
Ru(2)–S(1)	2.3821(10)
Ru(3)–S(1)	2.3795(11)
Ru(1)–C(7)	2.197(4)
Ru(2)–C(7)	2.180(4)
Ru(3)–C(7)	2.154(4)
O(1)–C(1)	1.150(5)
N(1)–C(33)	1.355(5)
N(2)–C(33)	1.345(5)
N(1)–C(35)	1.464(6)
N(1)–C(34)	1.461(6)
Ru(1)–P(1)	2.3419(11)
Ru(2)–P(2)	2.3211(11)
P(1)–C(20)	1.842(4)
P(2)–C(20)	1.831(4)
Ru(1)–Ru(3)–Ru(2)	59.258(10)
Ru(2)–Ru(1)–Ru(3)	60.515(10)
Ru(1)–Ru(2)–Ru(3)	60.227(10)
Ru(1)–S(1)–Ru(3)	72.62(3)
Ru(3)–S(1)–Ru(2)	72.72(3)
Ru(1)–S(1)–Ru(2)	71.75(3)
Ru(3)–C(7)–Ru(1)	80.62(14)
Ru(2)–C(7)–Ru(1)	79.10(14)
C(7)–Ru(3)–Ru(1)	50.36(11)
C(7)–Ru(3)–Ru(2)	49.76(11)
C(7)–Ru(1)–Ru(2)	50.18(10)
S(1)–Ru(3)–Ru(2)	53.68(2)
S(1)–Ru(1)–Ru(2)	54.25(2)
S(1)–Ru(3)–Ru(1)	53.61(2)
S(1)–Ru(2)–Ru(1)	54.00(2)
S(1)–Ru(2)–Ru(3)	53.60(3)
S(1)–Ru(1)–Ru(3)	53.77(3)
P(2)–Ru(2)–Ru(1)	90.00(3)
P(1)–Ru(1)–Ru(2)	94.95(3)
P(2)–C(20)–P(1)	111.7(2)
N(1)–C(33)–Ru(3)	122.5(3)
N(2)–C(33)–N(1)	113.4(3)

The structure of **9** is therefore based on comparison of spectra with those of the corresponding mixed S–Se analogue **15**, the XRD structure of which we report in this paper. The IR spectra of **9** and **15** are very similar, indicating that they are isostructural. The FAB MS shows the molecular ion (*m/z* 1021) and the stepwise loss of up to six carbonyl groups. The ^{1}H NMR spectrum shows three multiplets at δ 7.48, 4.33, 3.83 and a singlet at δ 3.38 in a 20:1:1:12 intensity ratio assigned, respectively, to Ph, non-equivalent CH_2 protons of dppm and Me of $(Me_2N)_2C$.

The IR spectrum for **11** exhibits a bridging carbonyl band at 1740 cm^{-1} and the ^{1}H NMR spectrum in the aromatic region is characteristic of an orthometallated phenyl ring. The $^{31}P\{^1H\}$ NMR spectrum contains two doublets ($J = 102.0$ Hz) of equal intensity at δ 22.6 and 138.3 due to the magnetically non-equivalent ^{31}P nuclei of the ligand. The signal at δ 22.6 is due to the terminal phosphorus atom while the low field signal at δ 138.3 is characteristic of a phosphorus atom bridging a metal–metal bond. The ^{31}P chemical shifts are close to those reported for structurally characterized orthometallated compound $[Ru_3\{\mu_3\text{-}\eta^3\text{-}PhPCH_2PPh(C_6H_4)\}(CO)_9]$ [δ 2.9 (d), 117.3 (d), J = 85.0 Hz)], [9] suggesting the presence of a μ_3-η^3-$PhPCH_2PPh(C_6H_4)$ ligand in **11**. The mass spectrum shows the parent at *m/z* 885 and fragments ions formed by the sequential loss of one Ph and seven carbonyl groups. Most probably **11** is formed by the reaction of the orthometallated compound $[Ru_3\{\mu_3\text{-}\eta^3\text{-}PhPCH_2PPh(C_6H_4)\}(CO)_9]$, formed in situ from the thermolysis of **4,** with selenium but we have not demonstrated this.

The solid-state molecular structure of **15** (Fig. 6 and Table 6) consists of an open Ru_3 triangle with six terminal carbonyl groups, a triply-bridging S, a triply-bridging Se, a bridging dppm and a tetramethyldiaminocarbene ligand. As with **8**, the tetramethyldiaminocarbene ligand is derived from C=S cleavage in the tetramethylthiourea ligand. Compound **15** is simply a tetramethyldiaminocarbene-substitution product of **14** but the replacement of CO by the carbene has significantly affected the geometry. There appears to be complete disorder between S and Se in compound **15** and the model was refined with 50% of each atom with identical coordinates in each site. The dppm coordination has shifted from the open metal–metal edge to the bonded Ru(1)–Ru(2) edge with Ru–P distances [Ru(1)–P(2) = 2.329(2) Å and Ru(2)–P(1) = 2.318(2) Å] similar to those in **4**. The dppm-bridged Ru(1)–Ru(2) distance of 2.7801(16) Å is significantly shorter than the nonbridged Ru(2)–Ru(3) distance of 2.8313(15) Å. The diaminocarbene ligand is coordinated equatorially to Ru(3) and the Ru(3)–C(1) distance of 2.078(7) Å is shorter than the corresponding distance in **8** but very similar to the osmium–carbene distance in $[Os_3(\mu\text{-}H)(CO)_8\{\mu\text{-}\eta^3\text{-}CN(Me)C(Et)C(Ph)C(Ph)\}]$ [2.07(1) Å] [36]. The carbene C–N bond lengths are similar to those in **8**. The μ_3-S ligand is bonded symmetrically with the three Ru–S distances in the range 2.4904(8)–2.5083(7) Å, whereas μ_3-Se ligand caps the Ru_3 core asymmetrically with the three Ru–Se distances ranging from 2.4648(15) to 2.5242(16) Å.

The IR spectrum of **15** shows only terminal carbonyl groups. The $^{31}P\{^1H\}$ NMR spectrum contains two doublets at δ 23.6 and 14.2, indicating non-equivalent ^{31}P nuclei. The mass spectrum shows the parent at *m/z* 1068. Compound **15** provides the first example of a structurally characterized 50-electron triruthenium cluster containing capping S/Se and a diphosphine bridging a bonded pair of Ru atoms. The coordination of the dppm ligand is structurally similar to that which has recently been reported for the 50-electron compound $[Os_3(\mu_3\text{-}Se)_2(CO)_7(\mu\text{-}dppm)]$ [38].

3. Conclusions

Our results on the treatment of **4** with tetramethylthiourea are summarised in Scheme 4 while those with elemental Se are in Scheme 6. Compounds **6** and **14** have bicapped open triangular structures with *nido* Ru_3EE' cores (**6**,

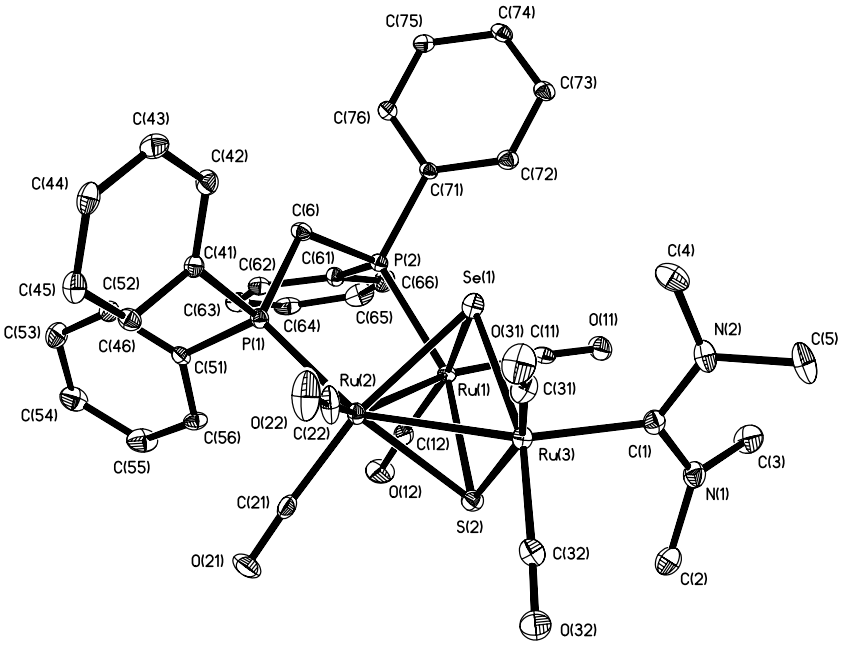

Fig. 6. Molecular structure of $[Ru_3(\mu_3\text{-}S)(\mu_3\text{-}Se)\{\eta^1\text{-}C(NMe_2)_2\}(CO)_6(\mu\text{-dppm})]$ (**15**).

Table 6
Selected bond distances (Å) and angles (°) for $[Ru_3(\mu_3\text{-}S)(\mu_3\text{-}Se)\{\eta^1\text{-}C(NMe_2)_2\}(CO)_6(\mu\text{-dppm})]$ (**15**)

Ru(1)–Ru(2)	2.7808(16)
Ru(2)–Ru(3)	2. 8313(15)
Ru(1)–S(1)/Se(1)	2.4904(18)
Ru(1)–S(2)/Se(2)	2.4648(15)
Ru(2)–S(1)/Se(1)	2.5083 (17)
Ru(2)–S(2)/Se(2)	2.5242(16)
Ru(3)–S(2)/Se(2)	2.4803(17)
Ru(3)–S(1)/Se(1)	2.5028(17)
Ru(1)–P(2)	2.329(2)
Ru(2)–P(1)	2.318 (2)
Ru(3)–C(1)	2.078(7)
N(1)–C(3)	1.479(10)
N(2)–C(1)	1.348(10)
N(2)–C(5)	1.486(10)
N(2)–C(4)	1.443(12)
N(1)–C(1)	1.367(10)
N(1)–C(2)	1.461(11)
Ru(1)–S(2)/Se(2)–Ru(2)	67.72(5)
Ru(1)–S(1)/Se(1)–Ru(2)	67.58(4)
Ru(1)–S(2)/Se(2)–Ru(3)	98.36(6)
Ru(3)–S(2)/Se(2)-Ru (2)	68.90(4)
S(2)/Se(2)–Ru(1)–Ru(2)	57.16(3)
S(1)/Se(1)–Ru(1)–Ru(2)	56.52(4)
S(1)/Se(1)–Ru(2)–Ru(1)	55.90(5)
S(2)/Se(2)–Ru(2)–Ru(3)	54.82(3)
S(2)/Se(2)–Ru(3)–Ru(2)	56.28 (4)
S(1)/Se(1)–Ru(2)–Ru(3)	55.51(4)
P(2)–Ru(1)–Ru(2)	99.23(5)
P(1)–Ru(2)–Ru(1)	87.16(6)
Ru(1)–Ru(2)–Ru(3)	83.56(5)
C(1)–Ru(3)–Ru(2)	144.65(19)
N(2)–C(1)–N(1)	114.1(7)
S(2)/Se(2)–Ru(2)–Ru(1)	55.12(4)
Ru(3)–S(1)/Se(1)–Ru(2)	68.80(5)
Ru(1)–S(1)/Se(1)–Ru(3)	97.09(7)
S(1)/Se(1)–Ru(3)–Ru(2)	55.69(4)

E = E′ = S; **14**, E = S, E′ = Se). A dppm spans the non-bonded metal–metal edge. The structures could be described as a square pyramid with two Ru and two S/Se alternating in the basal plane with the third Ru atom at the apex. In sharp contrast to the reaction of **1** with tetramethylthiourea which affords two isomeric forms of the *nido* cluster $[Os_3(\mu\text{-}S)_2(CO)_7(\mu\text{-dppm})]$, the reaction of **4** with tetramethylthiourea gives four triruthenium clusters **5** to **8** containing bridging dppm and capping S ligands, the latter from C=S bond cleavage. Compounds **7** and **10** contain μ_3-CO on one face and a μ_3-S or Se on the opposite face and a bridging dppm. They both display tetrahedral Ru_3E (E = S or Se) cores. Compound **8** represents an unusual example of a S-capped Ru_3 cluster containing a diaminocarbene ligand. Cluster **7** can formally be derived from **8** by replacement of the diaminocarbene ligand by CO.

In contrast to the reaction of elemental Se with **1** which gave intractible materials, it reacts with **4** to give three new Ru_3 selenido clusters **10**–**12** and the previously reported cubane cluster **13**. Further reaction of **10** with elemental Se does not produce $[Ru_3(\mu_3\text{-}Se)_2(CO)_7(\mu\text{-dppm})]$ whereas with tetramethylthiourea the mixed S/Se compound **14** is formed.

4. Experimental

Although the products are air-stable, all reactions were performed under an atmosphere of nitrogen. THF, toluene, heptane and hexane were dried over sodium and distilled from sodium benzophenone ketyl under nitrogen immediately prior to use. Methylene chloride was freshly distilled from calcium hydride before use. IR spectra were recorded on a Shimadzu FTIR 1401 spectrometer, NMR spectra on a Bruker 400 or AM-300 or Varian Unity Plus

400 spectrometers. ^{31}P NMR chemical shifts are relative to 85% H_3PO_4 (external reference) and ^1H chemical shifts are referenced against residual protonated solvent. Fast atom bombardment mass spectra were obtained on a JEOL SX-102 spectrometer using 3-nitrobenzyl alcohol as matrix and CsI as calibrant. The cluster $[Ru_3(CO)_{10}(\mu\text{-dppm})]$ (**4**) was prepared by a published procedure [39].

4.1. Reaction of $[Ru_3(CO)_{10}(\mu\text{-dppm})]$ (4) with tetramethylthiourea

A THF solution (35 ml) of **4** (0.300 g, 0.31 mmol) and tetramethylthiourea (0.161 g, 1.22 mmol) was refluxed for 6 h. The solvent was pumped off and the residue chromatographed (TLC on silica gel). Elution with cyclohexane/CH_2Cl_2 (7:3, v/v) developed four bands. The first band afforded $[Ru_3(\mu\text{-H})_2(\mu_3\text{-S})(CO)_7(\mu\text{-dppm})]$ (**5**) (0.017 g, 6%) as red crystals from CH_2Cl_2/hexane at room temperature. The second band yielded $[Ru_3(\mu_3\text{-S})_2(CO)_7(\mu\text{-dppm})]$ (**6**) (0.030 g, 10%) as red crystals from hexane/CH_2Cl_2 at −20 °C (Anal. Calc. for $C_{32}H_{22}O_7P_2Ru_3S_2$: C, 40.55; H, 2.34. Found: C, 40.65; H, 2.78%). IR (νCO, CH_2Cl_2): 2054s, 2016s, 1984m, 1971m cm^{-1}. ^1H NMR ($CDCl_3$): δ 7.36 (m, 20H), 3.14 (t, $J = 10.0$ Hz). $^{31}P\{^1H\}$ NMR ($CDCl_3$): δ 61.2 (s). FAB MS: m/z 949. The third band yielded $[Ru_3(\mu_3\text{-S})(CO)_7(\mu_3\text{-CO})(\mu\text{-dppm})]$ (**7**) (0.095 g, 32%) as yellow crystals from hexane/CH_2Cl_2 at −20 °C (Anal. Calc. for $C_{33}H_{22}O_8P_2Ru_3S$: C, 42.00; H, 2.35. Found: C, 42.15; H, 2.49%). IR (νCO, hexane): 2072s, 2026vs, 2007s, 1980m, 1736br cm^{-1}. ^1H NMR ($CDCl_3$): δ 7.34 (m, 20H), 3.92 (m, 1H), 3.57 (m, 1H). $^{31}P\{^1H\}$ NMR ($CDCl_3$): δ 30.2 (s). FAB MS: m/z 945 (M^+). The fourth band gave $[Ru_3(\mu_3\text{-S})\{\eta^1\text{-C}(NMe_2)_2\}(CO)_6(\mu_3\text{-CO})(\mu\text{-dppm})]$ (**8**) (0.028 g, 9%) as orange crystals from hexane/CH_2Cl_2 at 4 °C (Anal. Calc. for $C_{37}H_{34}N_2O_7P_2Ru_3S$: C, 43.74; H, 3.37; N, 2.76. Found: C, 43.98; H, 3.67; N, 2.82%). IR (νCO, CH_2Cl_2): 2021s, 1996vs, 1985m, 1954s, 1942w cm^{-1}. ^1H NMR (CD_2Cl_2): δ 7.32 (m, 20H), 3.88 (m, 1H), 3.44 (m, 1H), 3.26 (s, 3H). $^{31}P\{^1H\}$ NMR (CD_2Cl_2): δ 28.5 (s). FAB MS: m/z 1017.

4.2. Reaction of 4 with thiourea

A mixture of **4** (0.100 g, 0.103 mmol) and thiourea (0.015 g, 0.197 mmol) in THF (25 ml) was refluxed for 1 h. The solvent was pumped off and the residue chromatographed (TLC on silica gel). Elution with cyclohexane/CH_2Cl_2 (7:3, v/v) developed two bands affording **5** (0.029 g, 30%) and **7** (0.009 g, 10%).

4.3. Reaction of 7 with tetramethylthiourea

A THF solution (25 ml) of **7** (0.100 g, 0.103 mmol) and tetramethylthiourea (0.027 g, 0.204 mmol) was refluxed for 4 h. Chromatographic separation as above afforded unconsumed **7** (0.035 g), **6** (0.030 g, 30%), and a new compound $[Ru_3(\mu_3\text{-S})_2\{\eta^1\text{-C}(NMe_2)_2\}(CO)_6(\mu\text{-dppm})]$ (**9**) (0.009 g, 8%) (Anal. Calc. for $C_{36}H_{34}N_2O_6P_2Ru_3S_2$: C, 42.39; H, 3.36; N, 2.75. Found: C, 42.45; H, 3.65; N, 2.84%), IR (νCO, CH_2Cl_2): 2012s, 1987vs, 1973s, 1939s cm^{-1}; ^1H NMR ($CDCl_3$): δ 7.48 (m, 20H), 4.33(m, 1H), 3.83 (m, 1H) 3.38 (s, 12H). $^{31}P\{^1H\}$ NMR ($CDCl_3$): δ 28.1 (d, $J = 51.5$ Hz), 18.5 (d, $J = 51.5$ Hz). FAB MS: m/z 1021(M^+).

4.4. Thermolysis of 8

A THF solution (15 ml) of **8** (0.020 g, 0.019 mmol) was refluxed for 5 h. The solvent was pumped off and the residue chromatographed as above to give **7** (0.011 g, 55%).

4.5. Reaction of 4 with elemental selenium

A THF solution (35 ml) of **4** (0.200 g, 0.210 mmol) and elemental Se (0.032 g, 0.417 mmol) was refluxed under N_2 for 5 h. The solvent was pumped off and the residue chromatographed (TLC on silica gel). Elution with cyclohexane/CH_2Cl_2 (7:3, v/v) developed four bands. The first band yielded $[Ru_3(\mu_3\text{-Se})(CO)_7(\mu_3\text{-CO})(\mu\text{-dppm})]$ (**10**) (0.060 g, 29%) as orange crystals from hexane/CH_2Cl_2 at 5 °C (Anal. Calc. for $C_{33}H_{22}O_8P_2Ru_3Se$: C, 40.01; H, 2.24. Found: C, 40.23; H, 2.42%). IR (νCO, CH_2Cl_2): 2069s, 2023vs, 2000s, 1971m cm^{-1}. ^1H NMR ($CDCl_3$): δ 7.34 (m, 20H), 4.23 (m, 1H), 3.61 (m, 1H). $^{31}P\{^1H\}$ NMR ($CDCl_3$): δ 25.9 (s). Mass spectrum: m/z 991 (M^+). The second band gave $[Ru_3(\mu_3\text{-Se})(CO)_6(\mu\text{-CO})\{\mu_3\text{-}\eta^3\text{-}P(C_6H_5)CH_2P(C_6H_5)(C_6H_4)\}]$ (**11**) (0.010 g, 5%) as yellow needles from hexane/CH_2Cl_2 at 5 °C (Anal. Calc. for $C_{26}H_{16}O_7P_2Ru_3Se$: C, 35.30; H, 1.82. Found: C, 35.52; H, 2.02%). IR (νCO, CH_2Cl_2): 2079s, 2046vs, 2023vs, 2008w, 1992m cm^{-1}. ^1H NMR ($CDCl_3$): δ 7.53 (m, 14H), 3.89 (m, 1H), 3.38 (m, 1 H). $^{31}P\{^1H\}$ NMR ($CDCl_3$): δ 22.6 (d, $J = 102.0$ Hz), 138.3 (d, $J = 102.0$ Hz); FAB MS: m/z 885. The third and the fourth bands gave the known compounds $[Ru_3(\mu\text{-H})_2(\mu_3\text{-Se})(CO)_7(\mu\text{-dppm})]$ (**12**) (0.004 g, 2%) and $[Ru_4(\mu_3\text{-Se})_4(CO)_{10}(\mu\text{-dppm})]$ (**13**) (0.003 g, 5%), respectively as yellow crystals from hexane/CH_2Cl_2 at 5 °C.

4.6. Reaction of 10 with tetramethylthiourea

A solution of **10** (0.100 g, 0.101 mmol) and tetramethylthiourea (0.027 g, 0.204 mmol) in THF (30 ml) was refluxed for 8 h. The solvent was pumped off and the residue chromatographed (TLC on silica gel). Elution with cyclohexane/CH_2Cl_2 (3:2, v/v) developed two bands. The major band afforded $[Ru_3(\mu_3\text{-S})(\mu_3\text{-Se})(CO)_7(\mu\text{-dppm})]$ (**14**) (0.038 g, 38%) as yellow crystals from CH_2Cl_2/hexane at −15 °C (Anal. Calc. for $C_{32}H_{22}O_7P_2Ru_3SSe$: C, 38.64; H, 2.23. Found: C, 38.81; H, 2.34%). IR (νCO, CH_2Cl_2): 2067w, 2052vs, 2016vs, 1986m, 1956m cm^{-1}. ^1H NMR ($CDCl_3$): δ 7.33 (m, 20H), 4.42 (m, 1H), 3.98 (m, 1H), 3.22 (t, 2H). $^{31}P\{^1H\}$ NMR ($CDCl_3$): major isomer δ 63.9 (s); minor isomer 24.8 (d, $J = 94.0$ Hz), 15.9 (d,

Table 7
Crystal data and structure refinement for **6**, **7**, **8**, **10**, **14** and **15**

Compound	**6**	**7**	**8** · CH_2Cl_2	**10**	**14**	**15**
Empirical formula	$C_{32}H_{22}O_7P_2Ru_3S_2$	$C_{33}H_{22}O_8P_2Ru_3S$	$C_{38}H_{36}Cl_2N_2O_7P_2Ru_3S$	$C_{33}H_{22}O_8P_2Ru_3Se$	$C_{32}H_{22}O_7P_2Ru_3SSe$	$C_{36}H_{34}N_2O_6P_2Ru_3SSe$
Formula weight	947.77	943.72	1100.80	990.62	994.67	1066.82
Temperature (K)	293(2)	150(2)	150(2)	150(2)	150(2)	150(2)
Crystal system	Monoclinic	Triclinic	Monoclinic	Triclinic	Monoclinic	Triclinic
Space group	*I*2/*a*	$P\bar{1}$	$P2_1/c$	$P\bar{1}$	*I*2/*a*	$P\bar{1}$
a (Å)	22.270(6)	9.056(2)	21.3770(3)	9.16270(10)	22.1940(5)	9.013(6)
b (Å)	14.331(3)	18.398(3)	9.1714(2)	10.12940(10)	14.0607(4)	10.550(7)
c (Å)	23..681(5)	22.148(5)	21.4585(4)	18.8287(3)	23.6310(7)	21.627(14)
α (°)	90	107.342(14)	90	96.9554(5)	90	77.491(10)
β (°)	111.580(17)	97.740(7)	97.1196(11)	101.4536(6)	111.6100(9)	79.943(11)
γ (°)	90	95.656(14)	90	94.5914(5)	90	81.770(11)
V (Å^3)	7028(3)	3452.6(12)	4174.65(13)	1690.38(4)	6856.0(3)	1965(2)
Z	8	4	4	2	8	2
$\text{Density}_{\text{calc}}$ (g cm^{-3})	1.791	1.816	1.751	1.946	1.927	1.803
Absorption coefficient (mm^{-1})	1.527	1.497	1.375	2.544	2.566	2.245
F(000)	3712	1848	2184	960	3856	1048
Crystal size (mm)	$0.35 \times 0.25 \times 0.12$	$0.20 \times 0.08 \times 0.06$	$0.28 \times 0.22 \times 0.20$	$0.18 \times 0.08 \times 0.07$	$0.25 \times 0.10 \times 0.05$	$0.57 \times 0.15 \times 0.08$
θ Range for data collection (°)	1.97–25.03	1.75–25.01	2.93–26.37	3.03–27.47	3.09–27.51	1.99–28.33
Limiting indices	$-25 \leqslant h \leqslant 25$	$-10 \leqslant h \leqslant 7$	$-26 \leqslant h \leqslant 26$	$-11 \leqslant h \leqslant 11$	$-28 \leqslant h \leqslant 28$	$-11 \leqslant h \leqslant 12$
	$-16 \leqslant k \leqslant 13$	$-20 \leqslant k \leqslant 20$	$-10 \leqslant k \leqslant 11$	$-13 \leqslant k \leqslant 13$	$-17 \leqslant k \leqslant 17$	$-13 \leqslant k \leqslant 13$
	$-26 \leqslant l \leqslant 25$	$-16 \leqslant l \leqslant 25$	$-24 \leqslant l \leqslant 26$	$-24 \leqslant l \leqslant 24$	$-30 \leqslant l \leqslant 30$	$-10 \leqslant l \leqslant 28$
Reflections collected	14159	11643	31985	29637	19084	16287
Independent reflections [R_{int}]	5337 [0.0641]	8415 [0.2359]	8506 [0.0834]	7652 [0.0411]	7751 [0.0416]	8800 [0.0549]
Maximum and minimum transmission			0.7705 and 0.6994	0.8420 and 0.6574	0.8824 and 0.5663	0.3611 and 0.8462
Data/restraints/parameters	5337/30/367	8415/0/751	8506/0/500	7652/0/424	7751/30/415	8800/0/466
Goodness-of-fit on F^2	1.010	0.988	0.975	1.164	1.010	0.722
Final *R* indices [$I > 2\sigma(I)$]	$R_1 = 0.0557$,	$R_1 = 0.0684$,	$R_1 = 0.0387$,	$R_1 = 0.0266$,	$R_1 = 0.0656$,	$R_1 = 0.0612$,
	$wR_2 = 0.1284$	$wR_2 = 0.1329$	$wR_2 = 0.0897$	$wR_2 = 0.0698$	$wR_2 = 0.1744$	$wR_2 = 0.1618$
R indices (all data)	$R_1 = 0.0708$,	$R_1 = 0.1210$,	$R_1 = 0.0573$,	$R_1 = 0.0326$,	$R_1 = 0.0859$,	$R_1 = 0.0839$,
	$wR_2 = 0.1317$	$wR_2 = 0.1373$	$wR_2 = 0.1048$	$wR_2 = 0.0879$	$wR_2 = 0.1819$	$wR_2 = 0.1849$
Largest difference peak and hole (e Å^{-3})	2.219 and −1.044	1.447 and −0.837	0.781 and −1.133	0.732 and −1.648	6.199 and −1.142	3.466 and −1.1807

$J = 94.0$ Hz); FAB MS: m/z 995. The minor band gave $[Ru_3(\mu_3\text{-}S)(\mu_3\text{-}Se)\{\eta^1\text{-}SC(NMe_2)_2\}(CO)_6(\mu\text{-dppm})]$ (**15**) (0.011 g, 10%) as yellow crystals from hexane/CH_2Cl_2 at 5 °C. (Anal. Calc. for $C_{36}H_{34}N_2O_6P_2Ru_3SSe$: C, 40.53; H, 3.21; N, 2.63. Found: C, 40.72; H, 3.34; N, 2.78%). IR (νCO, CH_2Cl_2): 2010s, 1987vs, 1970s, 1935s cm^{-1}; ^1H NMR ($CDCl_3$): δ 7.25 (m, 20H), 4.18(m, 1H), 3.97 (m, 1H) 3.33 (s, 12H). $^{31}P\{^1H\}$ NMR ($CDCl_3$): δ 23.6 (d, $J = 35.5$ Hz), 14.2 (d, $J = 35.5$ Hz); FAB MS: m/z 1068 (M^+).

4.7. X-ray crystallography

Intensity data for **6** and **7** were obtained using a Delft Instruments FAST TV area detector diffractometer using Mo Kα radiation ($\lambda = 0.71073$ Å) as described previously [40]. Data sets were corrected for absorption using DIFABS [41]. Crystal quality for **6** and **7** was poor, but their structures were satisfactory. Data for complexes **8**–**14** were obtained using a Bruker Nonius Kappa CCD diffractometer using Mo Kα radiation. Data collection and processing were carried out by using the programs COLLECT [42] and DENZO [43]. The data were corrected for absorption effects by comparing the symmetry related data using SORTAV [44]. Intensity data for **15** were obtained on a Bruker SMART APEX CCD diffractometer using Mo Kα radiation at 150(2) K. Data reduction and integration was carried out with SAINT+ and absorption corrections using SADABS [45,46].

The structures of **6** to **14** were solved by direct methods (SHELXS-96) [47] and refined on F^2 by full-matrix least squares (SHELXL-97) [48] using all unique data. SHELXTL PLUS V6.10 was used for structure solution and refinement for **15** [49]. For all structures, the nonhydrogen atoms were refined anisotropically and the hydrogen atoms were included in calculated positions (riding model). The phenyl rings in **6** and **7** were idealised. ISOR restraints were applied for C(122)–C(126) in **6** and O(6) in **7**. The Se and S positions in **14** were partially occupied with Se1/S1 and Se1′/S1′ sites being 0.83/0.17 and 0.17/0.83 occupied, respectively. Same positional parameters and temperature factor coefficients were refined for both partially occupied atoms at a given site using the EXYZ and EADP instructions in SHELXL-97. All non-hydrogen atoms in **15** were refined anisotropically and hydrogen atoms, except those bonded to Os, were placed in calculated positions (riding model). The positions of the hydrogen atoms bridging the Os atoms were refined using fixed isotropic thermal parameters.

The crystal data, details of data collection and refinement results are summarised in Table 7. Crystallographic data have been deposited with the Cambridge Crystallographic Data Centre, CCDC Nos 24852 for **6**, 244853 for **7**, 244854 for **8**, 244855 for **10**, 244856 for **14,** 244857 for **15**. Copies of this information may be obtained free of charge from the Director, CCDC, 12 Union Road, Cambridge, CB2 1EZ, UK, fax: +44 1223 336 033, email: deposit@ccdc.cam.ac.uk or on the web www: http://www.ccdc.ac.uk.

Acknowledgements

We thank Dr. K.M. Abdul Malik (Department of Chemistry, University of Cardiff) for obtaining X-ray data on compounds **6**–**14**. The Royal Society (London) and the Swedish Academy of Sciences are thanked for supporting the collaboration between AJD and EN and the Wenner-Gren Foundation (Stockholm) for a fellowship to A.J.D. to work at Lund University. SEK acknowledges support from the Royal Society (London), the Swedish International Development Agency and the Swedish Science Research Council.

References

[1] U. Bodensieck, H. Stoeckli-Evans, G. Süss-Fink, Chem. Ber. 123 (1990) 1603.
[2] U. Bodensieck, H. Stoeckli-Evans, G. Rheinwald, G. Süss-Fink, J. Organomet. Chem. 433 (1992) 167.
[3] U. Bodensieck, H. Stoeckli-Evans, G. Süss-Fink, J. Organomet. Chem. 433 (1992) 149.
[4] U. Bodensieck, J. Santiago, H. Stoeckli-Evans, G. Rheinwald, G. Süss-Fink, J. Chem. Soc., Dalton Trans. (1992) 255.
[5] U. Bodensieck, L. Hoferkamp, H. Stoeckli-Evans, G. Süss-Fink, J. Chem. Soc., Dalton Trans. (1993) 127.
[6] U. Bodensieck, H. Stoeckli-Evans, G. Süss-Fink, J. Chem. Soc., Chem. Commun. (1990) 267.
[7] U. Bodensieck, L. Hoferkamp, H. Stoeckli-Evans, G. Süss-Fink, Angew. Chem. 103 (1991) 1147;
Angew. Chem., Int. Ed. Engl. 30 (1991) 112.
[8] G. Süss-Fink, U. Bodensieck, L. Hoferkamp, G. Rheinwald, H. Stoeckli-Evans, J. Cluster Sci. 3 (1992) 469.
[9] U. Bodensieck, G. Meister, H. Stoeckli-Evans, G. Süss-Fink, J. Chem. Soc., Dalton Trans. (1992) 2131.
[10] E.W. Ainscough, A.M. Brodie, S.L. Ingham, G.G. Kotch, A.J. Lees, J. Lewis, J.M. Waters, J. Chem. Soc., Dalton Trans. (1994) 1.
[11] K.A. Azam, R. Dilshad, S.E. Kabir, R. Miah, M. Shahiduzzaman, E. Rosenberg, K.I. Hardcastle, M.B. Hursthouse, K.M.A. Malik, J. Cluster Sci. 7 (1996) 49.
[12] S.M.T. Abedin, K.A. Azam, M.B. Hursthouse, S.E. Kabir, K.M.A. Malik, R. Miah, H. Vahrenkamp, J. Organomet. Chem. 564 (1992) 133.
[13] N. Begum, A.J. Deeming, M.K. Islam, S.E. Kabir, D. Rokhsana, E. Rosenberg, J. Organomet. Chem. 689 (2004) 2633.
[14] K.A. Azam, G.M.G. Hossain, S.E. Kabir, K.M.A. Malik, Md.A. Mottalib, S. Pervin, N.C. Sarker, Polyhedron 21 (2002) 381.
[15] T. Akter, N. Begum, D.T. Haworth, D.W. Bennett, S.E. Kabir, Md.A. Miah, N.C. Sarker, T.A. Siddiquee, E. Rosenberg, J. Organomet. Chem. 689 (2004) 1569.
[16] A.K. Smith, in: E.W. Abel, F.G.A. Stone, G. Wilkinson (Eds)., Comprehensive Organometallic Chemistry II, vol. 7, Pergamon Press, Oxford, UK, 1995, p. 747, in: D.F. Shriver, M.I. Bruce (Eds.).
[17] E. Sappa, in: E.W. Abel, F.G.A. Stone, G. Wilkinson (Eds.), Comprehensive Organometallic Chemistry II, vol. 7, Pergamon Press, Oxford, UK, 1995, p. 804, in: D.F. Shriver, M.I. Bruce (Eds.).
[18] A.J. Deeming, in: E.W. Abel, F.G.A. Stone, G. Wilkinson (Eds.), Comprehensive Organometallic Chemistry II, vol. 7, Pergamon Press, Oxford, UK, 1995, p. 684, in: D.F. Shriver, M.I. Bruce (Eds.).
[19] (a) G. Lavigne, N. Lugan, J.-J. Bonnet, Organometallics 1 (1982) 1040; (b) N. Lugan, J.-J. Bonnet, J.A. Ibers, J. Am. Chem. Soc. 107 (1985) 4484;

(c) G. Lugan, J.-J. Bonnet, J.A. Ibers, Organometallics 7 (1988) 1538;
(d) G. Lavigne, J.-J. Bonnet, Inorg. Chem. 23 (1984) 952.
[20] C. Bergounhou, J.-J. Bonnet, P. Fompeyrine, G. Lavigne, N. Lugan, F. Mansilla, Organometallics 5 (1986) 60.
[21] D.F. Foster, J. Harrison, B.S. Nicholls, A.K. Smith, J. Organomet. Chem. 295 (1985) 99.
[22] C.J. Adams, M.I. Bruce, B.W. Skelton, A.H. White, J. Organomet. Chem. 430 (1992) 181, and references therein.
[23] M.I. Bruce, P.A. Humphrey, B.W. Skelton, A.H. White, J. Organomet. Chem. 429 (1992) 187.
[24] S.E. Kabir, M. Karim, K.M.A. Malik, T.A. Siddiquee, Inorg. Chem. Commun. 2 (1999) 128.
[25] P. Fompeyrine, G. Lavigne, J.-J. Bonnet, J. Chem. Soc., Dalton Trans. (1987) 91.
[26] M.I. Bruce, N.N. Zaitseva, B.W. Skelton, A.H. White, J. Organomet. Chem. 515 (1996) 143.
[27] (a) M.I. Bruce, P.A. Humphrey, E. Horn, E.R.T. Tiekink, B.W. Skelton, A.H. White, J. Organomet. Chem. 429 (1992) 207;
(b) M.I. Bruce, J.R. Hinchliffe, R. Surynt, B.W. Skelton, A.H. White, J. Organomet. Chem. 469 (1994) 89;
(c) M.I. Bruce, P.A. Humphrey, H. Miyamae, B.W. Skelton, A.H. White, J. Organomet. Chem. 429 (1992) 187.
[28] A.J. Deeming, Md.I. Hyder, S.E. Kabir, S.J. Ahmed, K.M.A. Malik, unpublished results.
[29] M.R. Churchill, F.J. Hollander, J.P. Hatchinson, Inorg. Chem. 16 (1977) 2655.
[30] T.M. Layer, J. Lewis, A. Martin, P.R. Raithby, W.-T. Wong, J. Chem. Soc., Dalton Trans. (1992) 1411.
[31] D. Cauzzi, C. Graiff, M. Chiara, G. Predieri, A. Tiripicchio, D. Acquotti, J. Chem. Soc., Dalton Trans. (1999) 3515.
[32] D. Cauzzi, C. Graiff, G. Predieri, A. Tiripicchio, C. Vignali, J. Chem. Soc., Dalton Trans. (1999) 237.
[33] D. Cauzzi, C. Graiff, M. Lanfranchi, G. Predieri, A. Tiripicchio, J. Chem. Soc., Dalton Trans. (1995) 2321.
[34] R.D. Adams, J.E. Babin, M. Tasi, Organometallics 7 (1988) 219.
[35] A.W. Coleman, D.F. Jones, P.H. Dixneuf, C. Brisson, J.-J. Bonnet, G. Lavigne, Inorg. Chem. 23 (1984) 952.
[36] R.D. Adams, G. Chen, Organometallics 11 (1992) 837.
[37] U. Schubert, in: K.H. Dötz, H. Fischer, P. Hoffmann, U. Schubert, K. Weiss (Eds.), Transition Metal Carbene Complexes, Verlag Chemie, Weinheim, Germany, 1983.
[38] S.E. Kabir, S. Pervin, N.C. Sarker, A. Yesmin, T.A. Siddiquee, D.T. Haworth, D.W. Bennett, K.M.A. Malik, J. Organomet. Chem. 681 (2003) 237.
[39] M.I. Bruce, B.K. Nicholson, M.L. Williams, Inorg. Synth. 26 (1989) 271;
Inorg. Synth. 28 (1990) 225.
[40] J.A. Darr, S.R. Drake, M.B. Hursthouse, K.M.A. Malik, Inorg. Chem. 32 (1993) 5704.
[41] N.P.C. Walker, D. Stuart, Acta Crystallogr. A39 (1983) 158.
[42] R. Hooft, COLLECT Data Collection Software, Nonius B.V. Delft, The Netherlands, 1998.
[43] Z. Otwinowski, W. Minor, in: C.W. Carter, R.M. Sweet (Eds.), Macromolecular Crystallography, Academic Press, New York, 1997, p. 307.
[44] R.H. Blessing, Acta Crystallogr. A51 (1995) 33.
[45] SMART and SAINT Software for CCD Diffractometers, version 6.1, Bruker AXS, Madison, WI, 2000.
[46] G.M. Sheldrick, SADABS Software for Empirical Absorption Correction, University of Göttingen, Germany, 2000.
[47] G.M. Sheldrick, Acta Crystallogr. A46 (1990) 467.
[48] G.M. Sheldrick, SHELXL-97, Program for Crystal Structure Refinement, University of Göttingen, Germany, 1997.
[49] G.M. Sheldrick, SHELXTL PLUS, Version 6.1, Bruker AXS Inc., Madison, WI, 2000.